*Korean J. Chem. Eng.*, **27**(6), 1755-1759 (2010)
DOI: 10.1007/s11814-010-0279-3

# Production of middle distillate through hydrocracking of paraffin wax over $NiMo/TiO_2$-$SiO_2$ catalysts

**Joongwon Lee*, Sunhwan Hwang*, Sang-Bong Lee**, and In Kyu Song*,†**

*School of Chemical and Biological Engineering, Institute of Chemical Processes, Seoul National University, Shinlim-dong, Kwanak-gu, Seoul 151-744, Korea
**Korea Research Institute of Chemical Technology, Daejeon 305-600, Korea
(*Received 9 February 2010 • accepted 2 March 2010*)

**Abstract**−Titania-silica (TS(X), X=19, 26, 55, 70, and 79) supports with different titania content (X, wt%) were prepared by a precipitation method. NiMo/TS(X) catalysts prepared by an incipient wetness method were then applied to the production of middle distillate through hydrocracking of paraffin wax. Successful formation of NiMo/TS(X) (X=19, 26, 55, 70, and 79) catalysts was confirmed by ICP-AES and XRD measurements. $NH_3$-TPD experiments were conducted to measure the acid property of NiMo/TS(X) (X=19, 26, 55, 70, and 79) catalysts. It was revealed that acidity of the catalyst played an important role in determining the catalytic performance in the hydrocracking of paraffin wax. Conversion of paraffin wax increased with increasing acidity of the catalyst, while yield for middle distillate showed a volcano-shaped curve with respect to acidity of the catalyst. Among the catalysts tested, NiMo/TS(26) retaining moderate acidity showed the highest yield for middle distillate.

Key words: Hydrocracking, Middle Distillate, Titania-silica, Acid Property, NiMo Catalyst

## INTRODUCTION

Hydrocracking has been an important industrial process for the production of gasoline and middle distillate from heavy hydrocarbons [1-3]. Crude oil has been conventionally used as a source of the hydrocracking process for the production of middle distillate [4]. Fischer-Tropsch (FT) wax has also attracted much attention as a source of the hydrocracking process, because it can produce high quality middle distillate compared to crude oil. FT wax is typically composed of *n*-paraffins (>90%), alcohols, and olefins. Furthermore, FT wax retains low sulfur and aromatic compounds, resulting in clean burning feature in compression-ignition engines [5].

Hydrocracking is generally conducted over a bifunctional (metal/acid) catalyst [6-11]. Metal sites provide hydrogenation-dehydrogenation function and acidic sites provide cracking function through carbocationic mechanism. The most conventional catalysts used for the production of gasoline or diesel from crude oil are NiMo and NiW catalysts supported on alumina and silica-alumina [12-16]. Titania-silica can also be potentially available as a support for hydrotreating catalyst due to its favorable physicochemical properties. It is expected that the combination of titania and silica not only generates strong acid sites but also provides enhanced thermal and mechanical stability [17-21].

In this work, a series of $TiO_2$-$SiO_2$ supports with different composition were prepared by a precipitation method, with an aim of controlling the acid property of $TiO_2$-$SiO_2$. $NiMo/TiO_2$-$SiO_2$ catalysts were prepared by an incipient wetness method and then sulfided for use in the production of middle distillate through hydrocracking of paraffin wax. $NH_3$-TPD experiments were conducted to investigate the effect of support composition on the acid property of $NiMo/TiO_2$-$SiO_2$ catalysts. The acid property of $NiMo/TiO_2$-$SiO_2$ catalysts was then correlated with their catalytic performance in the hydrocracking of paraffin wax.

†To whom correspondence should be addressed.
E-mail: inksong@snu.ac.kr

## EXPERIMENTAL

### 1. Catalyst Preparation

$TiO_2$-$SiO_2$ supports with different $TiO_2$ content were prepared by a precipitation method. A known amount of titanium isopropoxide ($Ti(OCH(CH_3)_2)_4$, Sigma-Aldrich) and tetraethylorthosilicate ($Si(OC_2H_5)_4$, Sigma-Aldrich) was separately dissolved in 2-propanol ($C_3H_7OH$, Sigma-Aldrich). An appropriate amount of acetylacetone ($C_5H_8O_2$, Sigma-Aldrich) was added into the solution containing titanium precursor. These two precursor solutions were then mixed with vigorous stirring to form a homogeneous solution. A known amount of distilled water was added dropwise into the mixed solution for precipitation. After filtering and washing a solid product with 2-propanol, the solid product was dried overnight at 100 °C. The resulting solid was finally calcined at 550 °C for 3 h to yield a $TiO_2$-$SiO_2$ support. The prepared $TiO_2$-$SiO_2$ supports were denoted as TS(X) (X=19, 26, 55, 70, and 79), where X is wt% of $TiO_2$ in $TiO_2$-$SiO_2$.

NiMo catalysts supported on $TiO_2$-$SiO_2$ were prepared by an incipient wetness method using a mixed aqueous solution containing ammonium molybdate tetrahydrate ($(NH_4)_6Mo_7O{\cdot}4H_2O$, Samchun) and nickel nitrate hexahydrate ($Ni(NO_3)_2{\cdot}6H_2O$, Fluka). In all the supported catalysts, NiO and $MoO_3$ loadings were adjusted at ca. 5 and ca. 21 wt%, respectively. After the impregnated catalysts were dried overnight at 110 °C, they were calcined at 500 °C for 3 h. The prepared $NiMo/TiO_2$-$SiO_2$ catalysts were denoted as NiMo/TS(X) (X=19, 26, 55, 70, and 79). All the catalysts were sulfided in a fixed-

bed reactor by flowing a mixed stream (34,283 ml/h·g) of $H_2S$ (10%) and $H_2$ (90%) at 360 °C for 3 h under atmosphere pressure, prior to use in catalytic reaction.

**2. Characterization**

Composition of NiO, $MoO_3$, and $TiO_2$ in the prepared catalyst was determined by ICP-AES measurement (Shimadzu, ICP-1000IV). Surface area of the catalyst was measured using a BET apparatus (Micromeritics, ASAP 2010). Crystalline phase of the catalyst was investigated by XRD measurement (Rigaku, D-MAX2500-PC) using Cu-K$\alpha$ radiation ($\lambda$=1.54056 Å) operated at 50 kV and 100 mA. High resolution-transmission electron microscopy (HR-TEM) analysis (Jeol, JEM-3010) was conducted to examine the morphology of sulfided catalyst.

$NH_3$-TPD experiment was conducted to determine the acid property of sulfided catalyst (BEL Japan, BELCAT-B). For the TPD measurement, each catalyst was pretreated at 200 °C for 1 h under a flow of helium (50 ml/min) to remove any physisorbed organic molecules. $NH_3$ (50 ml/min) was then introduced into the reactor at 50 °C for 30 min, until the acid sites were saturated with $NH_3$. Physisorbed $NH_3$ was removed at 150 °C for 1 h under a flow of helium (50 ml/min). After the sample was cooled, the furnace temperature was increased from room temperature to 850 °C at a heating rate of 5 °C/min under a flow of helium (30 ml/min). The desorbed $NH_3$ was detected by using a TCD (thermal conductivity detector).

**3. Hydrocrackig of Paraffin Wax**

Hydrocracking of paraffin wax to produce middle distillate was carried out over sulfided NiMo/TS(X) catalysts in a stainless steel autoclave reactor (75 ml). 0.7 g of sulfided catalyst and 18 g of paraffin wax (Sigma-Aldrich) were charged into the reactor at room temperature. After being purged with nitrogen several times, the reactor was pressurized to 35 bar with hydrogen and then heated to a reaction temperature of 400 °C. The reaction was conducted for 2 h at hydrogen pressure of 60 bar. The products were analyzed with gas chromatographs (Younglin 600D and Younglin ACME 6100). Carbon number distribution of paraffin wax reactant (melting point: 58-62 °C, ASTM D87) was in the range of $C_{21}$-$C_{34}$, as listed in Table 1. Wax conversion and product selectivity were calculated according to the Eqs. (1)-(4). Yield for middle distillate was calculated by multiplying conversion of wax and selectivity for middle distillate.

$$\text{Wax } (C_{21+}) \text{ conversion } (\%) = \frac{\text{wt\% of } C_{21+} \text{ in the feed} - \text{wt\% of } C_{21+} \text{ in the product}}{\text{wt\% of } C_{21+} \text{ in the feed}} \times 100 \quad (1)$$

$$C_1\text{-}C_4 \text{ selectivity } (\%) = \frac{\text{wt\% of } C_1\text{-}C_4 \text{ in the product}}{\text{wt\% of } C_{21+} \text{ in the feed} - \text{wt\% of } C_{21+} \text{ in the product}} \times 100 \quad (2)$$

$$C_5\text{-}C_9 \text{ selectivity } (\%) = \frac{\text{wt\% of } C_5\text{-}C_9 \text{ in the product}}{\text{wt\% of } C_{21+} \text{ in the feed} - \text{wt\% of } C_{21+} \text{ in the product}} \times 100 \quad (3)$$

**Table 2. Characterization results of NiMo/TS(X) (X=19, 26, 55, 70, and 79) catalysts**

| Catalyst | NiO (wt%)[a] | $MoO_3$ (wt%)[a] | $TiO_2$ (wt%)[a] | BET surface area ($m^2$/g) |
|---|---|---|---|---|
| NiMo/TS(19) | 5.0 | 22.0 | 19 | 227 |
| NiMo/TS(26) | 4.7 | 21.2 | 26 | 147 |
| NiMo/TS(55) | 4.9 | 21.4 | 55 | 61 |
| NiMo/TS(70) | 4.7 | 21.0 | 70 | 49 |
| NiMo/TS(79) | 4.8 | 20.9 | 79 | 27 |

[a]Determined by ICP-AES measurement

$$C_{10}\text{-}C_{20} \text{ (middle distillate) selectivity } (\%) = \frac{\text{wt\% of } C_{10}\text{-}C_{20} \text{ in the product}}{\text{wt\% of } C_{21+} \text{ in the feed} - \text{wt\% of } C_{21+} \text{ in the product}} \times 100 \quad (4)$$

## RESULTS AND DISCUSSION

**1. Physicochemical Properties of NiMo/TS(X) Catalysts**

Chemical composition and BET surface area of NiMo/TS(X) (X=19, 26, 55, 70, and 79) catalysts are summarized in Table 2. Chemical composition of NiO and $MoO_3$ determined by ICP-AES analyses was in good agreement with the designed value, indicating that all the supported catalysts were successfully prepared. $TiO_2$ content in the NiMo/TS(X) (X=19, 26, 55, 70, and 79) catalysts was controlled to be distributed within the wide range of 19-79 wt%, in order to investigate the effect of support composition on the acid property and catalytic performance of NiMo/TS(X) (X=19, 26, 55, 70, and 79) catalysts. BET surface area of the catalysts decreased with increasing $TiO_2$ content. This result was well consistent with the previous work [22] reporting that the increase of Ti content favors the formation of pure titania, leading to the decrease of BET surface area.

**2. Crystalline Phase and Morphology of NiMo/TS(X) Catalysts**

Fig. 1 shows the XRD patterns of TS(X) (X=19, 26, 55, 70, and 79) supports calcined at 550 °C. Each crystalline phase was indentified by JCPDS. A weak and broad peak was observed at around $2\theta$=25°, when titania content was less than 79 wt%. This result indicates that titania was mixed with silica on an atomic scale, which prevented the separation and crystallization of titania even for the sample with high titania content. When titania content reached 79 wt%, characteristic diffraction peaks appeared at $2\theta$=25.2°, 37.9°, 48.0°, 55.0°, and 62.9°, indicative of anatase $TiO_2$. Fig. 2 shows the XRD patterns of NiMo/TS(X) (X=19, 26, 55, 70, and 79) catalysts sulfided at 360 °C. $MoS_2$ phase, which serves as an active site in the hydrocracking of paraffin wax, was observed in all the sulfided catalysts. However, Ni-Mo-S phase, which also serves as an active site in the hydrocracking of paraffin wax, was not detected in all the catalysts. This result indicates that Ni-Mo-S particles were finely dispersed on the supports by forming small Ni-Mo-S particles that

**Table 1. Carbon number distribution of paraffin wax**

| Carbon number | 21 | 22 | 23 | 24 | 25 | 26 | 27 | 28 | 29 | 30 | 31 | 32 | 33 | 34 |
|---|---|---|---|---|---|---|---|---|---|---|---|---|---|---|
| wt% | 0.4 | 1.0 | 2.8 | 5.5 | 9.1 | 11.3 | 11.8 | 10.9 | 9.7 | 8.7 | 10.4 | 10.3 | 7.8 | 0.3 |

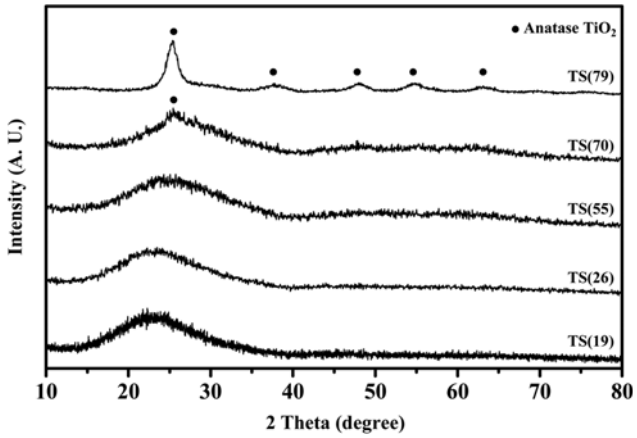


**Fig. 1. XRD patterns of TS(X) (X=19, 26, 55, 70, and 79) supports calcined at 550 °C.**

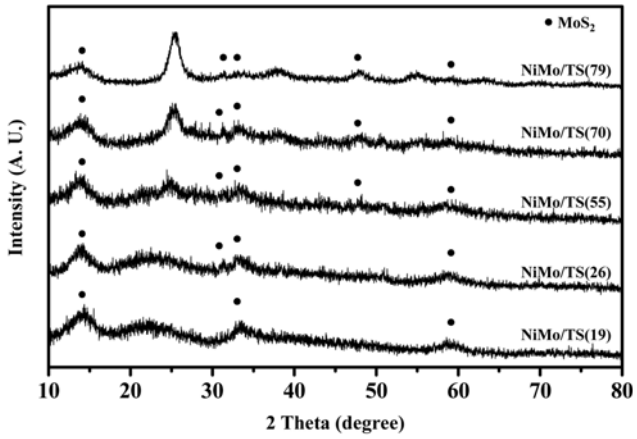


**Fig. 2. XRD patterns of NiMo/TS(X) (X=19, 26, 55, 70, and 79) catalysts sulfided at 360 °C.**

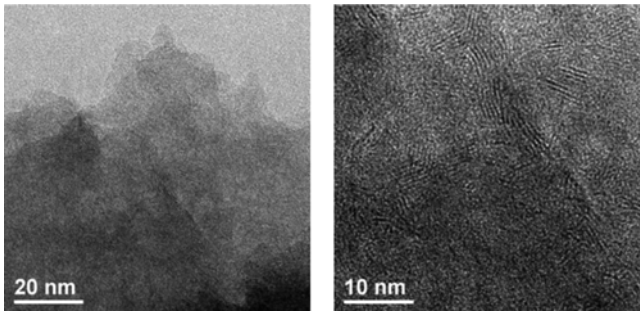


**Fig. 3. HR-TEM images of NiMo/TS(26) catalyst sulfided at 360 °C.**

were under detection limit of XRD measurement.

To investigate the morphologies of NiMo/TS(X) (X=19, 26, 55, 70, and 79) catalysts, HR-TEM analyses were conducted. Fig. 3 shows the HR-TEM images of NiMo/TS(26) catalyst sulfided at 360 °C. The images clearly show the layered structure of $MoS_2$ phase. It is known that the degree of slab length and stacked layers are affected by the sulfidation and dispersion of Ni and Mo species. It is also known that $MoS_2$ phase has a slab-like morphology and Ni

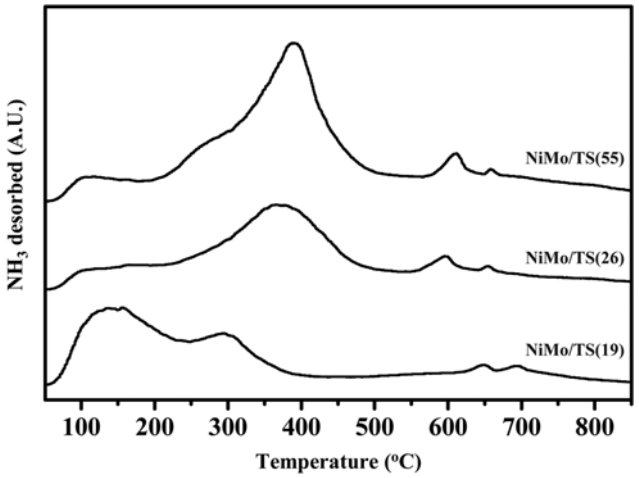


**Fig. 4. $NH_3$-TPD profiles of NiMo/TS(X) (X=19, 26, and 55) catalysts sulfided at 360 °C.**

**Table 3. Acidity of sulfided NiMo/TS(X) (X=19, 26, 55, 70, and 79) catalysts**

| Catalyst | Acidity (mmol-$NH_3$/g-catalyst) |
|---|---|
| NiMo/TS(19) | 0.131 |
| NiMo/TS(26) | 0.151 |
| NiMo/TS(55) | 0.223 |
| NiMo/TS(70) | 0.081 |
| NiMo/TS(79) | 0.032 |

atoms are located on the edge of $MoS_2$ sheet in the typical supported NiMo catalyst [23-25]. Therefore, it is inferred that the edges of these stacked layers serve as active sites in the hydrocracking of paraffin wax.

### 3. Acidity of NiMo/TS(X) Catalysts

To determine the acid property of NiMo/TS(X) (X=19, 26, 55, 70, and 79) catalysts, $NH_3$-TPD experiments were conducted over sulfided catalysts. Fig. 4 shows the $NH_3$-TPD profiles of NiMo/TS(X) (X=19, 26, and 55) catalysts sulfided at 360 °C. The acidity of sulfided NiMo/TS(X) (X=19, 26, 55, 70, and 79) catalysts is summarized in Table 3. The acidity of the catalysts showed a volcano-shaped trend with respect to $TiO_2$ content. Among the catalysts tested, NiMo/TS(55) exhibited the largest acidity.

### 4. Effect of Acid Property on Catalytic Performance

Catalytic performance of NiMo/TS(X) (X=19, 26, 55, 70, and 79) catalysts for hydrocracking of paraffin wax performed at 400 °C and 60 bar for 2 h is listed in Table 4. Fig. 5 shows the correlation between acidity and conversion of paraffin wax over NiMo/TS(X) (X=19, 26, 55, 70, and 79) catalysts. The correlation clearly shows that conversion of paraffin wax is closely related to the acid property of the catalyst. Conversion of paraffin wax increased with increasing acidity of the catalyst. This can be understood by the fact that hydrocracking ability of the catalyst increased with increasing acidity of the catalyst. This result indicates that the acidity of the catalyst served as a crucial factor determining the catalytic performance in the hydrocracking of paraffin wax. Although the surface area of the catalysts showed great difference (Table 2), the surface area exhibited no reliable correlation with the catalytic performance.

**Table 4. Catalytic performance of NiMo/TS(X) (X=19, 26, 55, 70, and 79) catalysts**

| Catalyst | $C_{21+}$ conversion | Product selectivity (%) | | | $C_{10}$-$C_{20}$ yield (%) |
|---|---|---|---|---|---|
| | | $C_1$-$C_4$ | $C_5$-$C_9$ | $C_{10}$-$C_{20}$ | |
| NiMo/TS(19) | 26.1 | 9.7 | 25.5 | 64.8 | 16.9 |
| NiMo/TS(26) | 31.5 | 10.2 | 27.2 | 62.6 | 19.7 |
| NiMo/TS(55) | 34.1 | 27.1 | 28.6 | 44.3 | 15.1 |
| NiMo/TS(70) | 19.1 | 9.2 | 24.6 | 66.2 | 12.7 |
| NiMo/TS(79) | 16.8 | 7.5 | 25.4 | 67.1 | 11.3 |

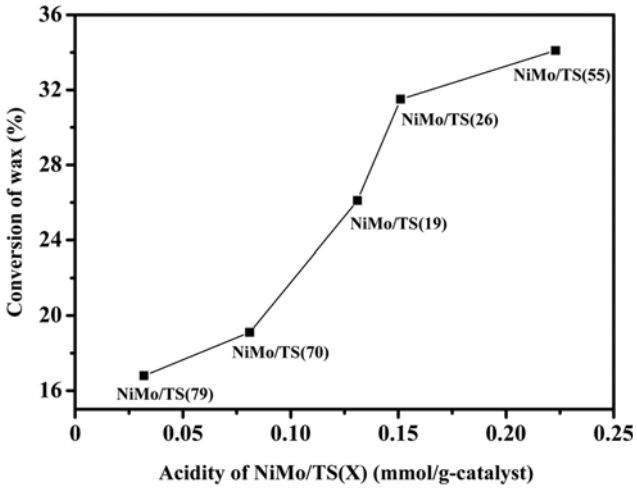


**Fig. 5. A correlation between acidity and conversion of paraffin wax over NiMo/TS(X) (X=19, 26, 55, 70, and 79) catalysts.**

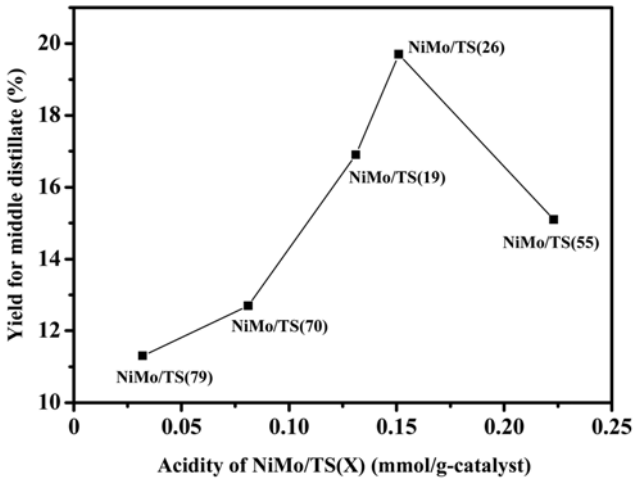


**Fig. 6. A correlation between acidity and yield for middle distillate over NiMo/TS(X) (X=19, 26, 55, 70, and 79) catalysts.**

Fig. 6 shows the correlation between acidity and yield for middle distillate over NiMo/TS(X) (X=19, 26, 55, 70, and 79) catalysts. Yield for middle distillate showed a volcano-shaped curve with respect to acidity. It has been reported that large acidity causes deep hydrocracking of paraffin wax and produces undesired light hydrocarbons ($<C_{10}$) [26]. For this reason, optimal acidity of NiMo/TS(X) catalyst was required for maximum production of middle distillate through hydrocracking of paraffin wax. Among the catalysts tested, NiMo/TS(26) catalyst with moderate acidity showed the highest yield for middle distillate.

## CONCLUSIONS

Titania-silica (TS(X)) supports with different titania content (X, wt%) were prepared by a precipitation method with an aim of controlling the acid property. NiMo catalysts supported on TS(X) (X=19, 26, 55, 70, and 79) were then prepared by incipient wetness method, and they were applied to the production of middle distillate through hydrocracking of paraffin wax. Successful formation of NiMo/TS(X) (X=19, 26, 55, 70, and 79) catalysts was well confirmed by ICP-AES and XRD measurements. $NH_3$-TPD experiments were conducted to measure the acidity of NiMo/TS(X) (X=19, 26, 55, 70, and 79) catalysts. Conversion of paraffin wax increased with increasing acidity of the catalyst, while yield for middle distillate showed a volcano-shaped curve with respect to acidity of the catalyst. Thus, the acidity of the catalyst served as a crucial factor determining the catalytic performance in the hydrocracking of paraffin wax. Among the catalysts tested, NiMo/TS(26) exhibited the highest yield for middle distillate. It is concluded that optimal acidity was required for maximum production of middle distillate through hydrocracking of paraffin wax.

## ACKNOWLEDGEMENTS

The authors would like to acknowledge funding from the Korea Ministry of Knowledge Economy (MKE) through "Energy Technology Innovation Program."

## REFERENCES

1. R. de Haan, G. Joorst, E. Mokoena and C. P. Nicolaides, *Appl. Catal. A*, **327**, 247 (2007).
2. L. Pellegrini, S. Bonomi, S. Gamba, V. Calemma and D. Molinari, *Chem. Eng. Sci.*, **62**, 5013 (2007).
3. M. A. Ali, T. Tatsumi and T. Masuda, *Appl. Catal. A*, **233**, 77 (2002).
4. H. Yang, C. Fairbridge, J. Hill and Z. Ring, *Catal. Today*, **93**, 457 (2004).
5. X. Huang, N. O. Elbashir and C. B. Roberts, *Ind. Eng. Chem. Res.*, **43**, 6369 (2004).
6. L. Leite, E. Benazzi and N. Marcheal-George, *Catal. Today*, **65**, 241 (2001).
7. K. Sato, Y. Iwata, T. Yoneda, A. Nishijima, Y. Miki and H. Shimada, *Catal. Today*, **45**, 367 (1998).
8. X. Dupain, R. A. Krul, M. Makkee and J. A. Moulijin, *Catal. Today*, **106**, 288 (2005).
9. S. Hwang, J. Lee, J. G. Seo, D. R. Park, M. H. Youn, J. C. Jung, S.-B. Lee and I. K. Song, *Catal. Lett.*, **132**, 410 (2009).
10. K. M. Cho, S. Park, J. G. Seo, M. H. Youn, S.-H. Baeck, K.-W. Jun, J. S. Chung and I. K. Song, *Appl. Catal. B*, **83**, 195 (2008).
11. K. M. Cho, S. Park, J. G. Seo, M. H. Youn, I. Nam, S.-H. Baeck, J. S. Chung, K.-W. Jun and I. K. Song, *Chem. Eng. J.*, **146**, 307 (2009).
12. I. Morawski and J. Mosie-Mosiewski, *Fuel Process. Technol.*, **87**, 659 (2006).
13. S. Hwang, J. Lee, S. Park, D. R. Park, J. C. Jung, S.-B. Lee and I. K.

Song, *Catal. Lett.*, **129**, 163 (2009).
14. M. S. Rana, S. K. Maity, J. Ancheyta, G. M. Dhar and T. S. R. P. Rao, *Appl. Catal. A*, **258**, 215 (2004).
15. M. Roussel, J.-L. Lemberton, M. Guisnet, T. Cseri and E. Benazzi, *J. Catal.*, **218**, 427 (2010).
16. Y. Rezgui and M. Guemini, *Appl. Catal. A*, **282**, 45 (2005).
17. Z. Liu, J. Tabora and R. J. Davis, *J. Catal.*, **149**, 117 (1994).
18. D. C. M. Dutoit, M. Schneider and A. Baikaer, *J. Catal.*, **153**, 165 (1995).
19. M. Breysse, J. L. Portefaix and M. Vrinat, *Catal. Today*, **10**, 489 (1991).
20. X. Gao and I. E. Wachs, *Catal. Today*, **51**, 233 (1999).
21. J. R. Sohn, H. J. Jang, M. Y. Park, E. H. Park and S. E. Park, *J. Mol. Catal.*, **93**, 149 (1994).
22. Y. Zhao, L. Xu, Y. Wang, C. Gao and D. Liu, *Catal. Today*, **93**, 583 (2004).
23. L. Ding, Y. Zheng, Z. Zhang, Z. Ring and J. Chen, *Appl. Catal. A*, **319**, 25 (2007).
24. C. Leyva, M. S. Rana and J. Ancheyta, *Catal. Today*, **130**, 345 (2008).
25. L. Qu, W. Zhang, P. J. Kooyman and R. Prins, *J. Catal.*, **215**, 7 (2003).
26. Y. Liu, K. Murata, K. Okabe, M. Inaba, I. Takahara, T. Hanaoka and K. Sakanishi, *Top. Catal.*, **52**, 597 (2009).